Available online at www.sciencedirect.com
SCIENCE DIRECT®
PERGAMON
International Journal of Heat and Mass Transfer 46 (2003) 3529–3537
International Journal of HEAT and MASS TRANSFER
www.elsevier.com/locate/ijhmt

Control of laminar natural convection in differentially heated square enclosures using solid inserts at the corners

V.A.F. Costa *, M.S.A. Oliveira, A.C.M. Sousa

Departamento de Engenharia Mecânica, Universidade de Aveiro, Campus Universitário de Santiago, Aveiro 3810-193, Portugal

Received 1 August 2002

Abstract

Solid inserts located at the corners of differentially heated two-dimensional square enclosures with laminar natural convection are used to control the heat rate within the enclosures. This numerical study employs air as the working fluid, and the variables of interest are the number, location, size and thermal conductivity of the triangular cross-section inserts. The major finding is that significant changes on the thermal performance of the enclosures can be achieved by using the inserts, which, when appropriately selected, can act either as heat transfer enhancers or as insulators. Analyses of the results, when the overall Nusselt number is the assessment parameter, show that it is viable, based on the variables of interest, to optimise the thermal performance of the enclosure.

1. Introduction

Natural convection in enclosures, and, in particular, natural convection in rectangular or square enclosures, is a widely studied problem [1,2], among many reasons, the interest stems from its ''richness'' in heat transfer and fluid mechanics features, such as, to name a few, recirculation and stagnation regions, boundary layers, jet deflection, and thermal entrainment. Therefore, it is not surprising these configurations are often used as benchmarking tests for CFD development [3,4]. Also, much work related to the thermal performance of such enclosures is available in the literature e.g. [5], where enhanced thermal performance implies increased or decreased overall heat transfer, depending on the goal, i.e. having the enclosure to act as a heat transfer promoter or as a thermal insulator, respectively.

When the goal is to reduce the heat transfer across the enclosure, ''baffles'' or fins (of finite or zero thermal conductivity) are usually employed, resulting in partitioned enclosures. The main effect is to trap the fluid, creating thermally stratified regions in rectangular [2,4,6,7] and in non-rectangular enclosures [8,9]. To this purpose, parallelogrammic enclosures were also considered. Sidewall angles and thermal boundary conditions are critical variables in what concerns insulation effects or heat transfer enhancement. Heat transfer can be substantially augmented by the use of such enclosures [10,11], where the parallelogrammic enclosure acts as a thermal diode. Other studies also considered the influence of thermally diffusive walls [8,9,11–15]. Heat transfer enhancement can also be achieved by creating an unsteady resonant heat transfer problem through the periodic change of the heating/cooling boundary conditions [16,17].

This work is addressed to the study of steady state, two-dimensional, laminar natural convection in square enclosures, and the objective is to study numerically the effect of solid inserts of triangular cross-section placed at selected corners of a square enclosure upon the thermal performance. The rationale for these inserts is to ''compensate'', if the target is to increase the heat transfer rate, with high thermal conductivity inserts the stagnation regions, which develop in the vicinity of the corners. It should be mentioned these stagnation regions, although to a lesser extent, are also common in the turbulent regime [18,19]. Obviously, inserts of thermal

* Corresponding author. Tel.: +351-234-370-829; fax: +351-234-370-953.
E-mail address: v_costa@mec.ua.pt (V.A.F. Costa).

0017-9310/03/$ - see front matter © 2003 Elsevier Science Ltd. All rights reserved.
doi:10.1016/S0017-9310(03)00141-8

Nomenclature

d	side length of the insert
g	gravitational acceleration
k	thermal conductivity
H	side length and height of the cavity
n	normal to the solid–fluid interface
Nu	Nusselt number
p	pressure
Pr	Prandtl number
Ra	Rayleigh number
Rc	thermal conductivity ratio
T	temperature
u, v	Cartesian velocity components
x, y	Cartesian co-ordinates

Greek symbols

α	thermal diffusivity
β	volumetric expansion coefficient
v	kinematic viscosity
ρ	density

Subscripts

c	pure conduction
C	cold wall
H	hot wall
f	fluid
o	overall
w	solid insert
0	reference value
$*$	dimensionless

conductivity lower than the fluid's will reduce the heat transfer rate. Also, as will be discussed, inserts with a thermal conductivity equal to the fluid, when their dimension exceeds the stagnation region, will reduce the heat transfer rate, simply because the advection process within the enclosure is inhibited.

There are different possible combinations for the placement of the inserts at the inner corners; however, exploratory studies only indicated three combinations of interest. For each case, all solid inserts have equal dimensions and thermal conductivity.

2. Mathematical and numerical modelling

2.1. Physical model

The domain under analysis is a two-dimensional square enclosure filled with air, and with differentially heated vertical walls. The horizontal walls are assumed to be perfect thermal insulators. The working fluid (air) is subjected to buoyancy effects, which set it into motion. Solid inserts are placed at selected corners, as depicted in Fig. 1. The solid inserts are made of non-zero thermal conductivity material, and its geometry is such that their cross-sections are triangles with angles of (90, 45, 45) degrees.

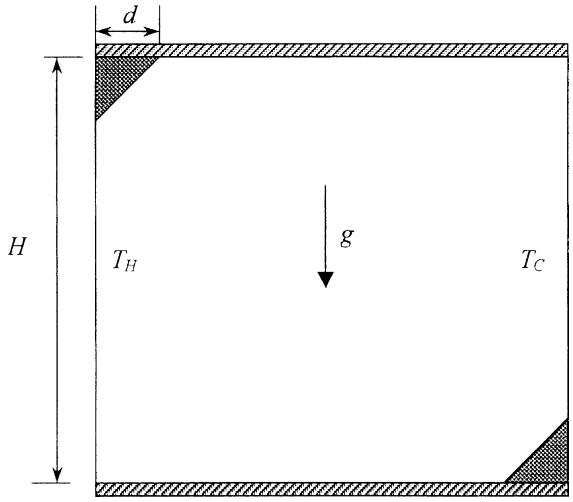

Fig. 1. Physical model and geometry.

2.2. Model assumptions

The enclosure is filled with a Newtonian-Fourier fluid, which flows in steady and laminar conditions and does not experience any phase change. This fluid is assumed to be incompressible but experiences density changes under the action of the temperature. This assumption leads to the Boussinesq approximation, if the maximum temperature difference is maintained within certain limits [20,21]. The fluid density is assumed to be constant throughout the governing equations, except for the buoyancy term, in which the density is taken as a function of the temperature with the thermal expansion coefficient, $\beta = -(\partial\rho/\partial T)_p/\rho$, taken as constant. All the thermal properties of the involved media (fluid and solid inserts) are assumed to be constant, except, as mentioned before, the density appearing in the buoyancy term.

The thermal levels and their differences within the enclosure are assumed to be sufficiently small to consider the effect of the thermal radiation upon the heat transfer

process to be negligible. The energy terms due to viscous dissipation and change of temperature due to reversible deformation (work of pressure forces) were also neglected.

2.3. Model equations

By introducing the dimensionless variables

$$u_* = uH/\alpha; \quad v_* = vH/\alpha \tag{1}$$

$$x_* = x/H; \quad y_* = y/H \tag{2}$$

$$T_* = (T - T_C)/(T_H - T_C) \tag{3}$$

and

$$p_* = (p + \rho_0 g y)/\lfloor \rho_0 (\alpha/H)^2 \rfloor \tag{4}$$

(where p_* is the dimensionless driving pressure), one obtains the following set of partial differential equations (Navier–Stokes equations) in normalized form, which governs the problem under analysis

$$\frac{\partial u_*}{\partial x_*} + \frac{\partial v_*}{\partial y_*} = 0 \tag{5}$$

$$\frac{\partial}{\partial x_*}(u_* u_*) + \frac{\partial}{\partial y_*}(v_* u_*) = -\frac{\partial p_*}{\partial x_*} + Pr\left(\frac{\partial^2 u_*}{\partial x_*^2} + \frac{\partial^2 u_*}{\partial y_*^2}\right) \tag{6}$$

$$\frac{\partial}{\partial x_*}(u_* v_*) + \frac{\partial}{\partial y_*}(v_* v_*) = -\frac{\partial p_*}{\partial y_*} + Pr\left(\frac{\partial^2 v_*}{\partial x_*^2} + \frac{\partial^2 v_*}{\partial y_*^2}\right) + Ra_H Pr\, T_* \tag{7}$$

The energy conservation for the fluid is given by the following normalized equation

$$\frac{\partial}{\partial x_*}(u_* T_*) + \frac{\partial}{\partial y_*}(v_* T_*) = \left(\frac{\partial^2 T_*}{\partial x_*^2} + \frac{\partial^2 T_*}{\partial y_*^2}\right) \tag{8}$$

and for the solid inserts

$$\frac{\partial^2 T_*}{\partial x_*^2} + \frac{\partial^2 T_*}{\partial y_*^2} = 0 \tag{9}$$

From the foregoing equations the dimensionless parameters emerge

$$Pr = \nu/\alpha \tag{10}$$

$$Ra_H = g\beta(T_H - T_C)H^3/\nu\alpha \tag{11}$$

The Prandtl, Eq. (10), and Rayleigh, Eq. (11), numbers are commonly used when analyzing natural convection heat transfer in enclosures filled with moderately small Prandtl number—fluids [2]. To study the effects of the inserts upon the heat transfer rates, two additional dimensionless parameters are required. They will be introduced under the discussion of the boundary conditions.

2.4. Boundary conditions

Over the walls of the cavity, the non-slip condition is imposed, namely,

$$u_*(0, y_*) = u_*(1, y_*) = u_*(x_*, 0) = u_*(x_*, 1) = 0 \tag{12}$$

$$v_*(0, y_*) = v_*(1, y_*) = v_*(x_*, 0) = v_*(x_*, 1) = 0 \tag{13}$$

as well as $u_* = v_* = 0$ over the solid inserts.

Over the vertical walls it is prescribed that

$$T_*(0, y_*) = 1; \quad T_*(1, y_*) = 0 \tag{14}$$

The problem under analysis is a conjugated heat transfer problem where, at each insert-fluid interface,

$$\left(-k\frac{\partial T}{\partial n}\right)_f = \left(-k\frac{\partial T}{\partial n}\right)_w \tag{15}$$

or, in a dimensionless form,

$$\left(\frac{\partial T_*}{\partial n_*}\right)_f = Rc\left(\frac{\partial T_*}{\partial n_*}\right)_w \tag{16}$$

where $Rc = k_w/k_f$ is the ratio between the thermal conductivity of the inserts and of the fluid that fills the cavity, and n is the direction normal to the solid–fluid interface. The thermal conductivity ratio, Rc, is one of the additional dimensionless parameters mentioned in the previous section. The other dimensionless parameter is related to the length of the solid inserts, which, in normalized form, is given as $d_* = d/H$. At any point of the solid–fluid (inserts) interface it is assumed that $T_f = T_w$. The horizontal boundaries of the enclosure are perfectly insulated, therefore

$$\left(\frac{\partial T_*}{\partial y_*}\right) = 0 \quad \text{for } y_* = 0 \text{ or } y_* = 1 \tag{17}$$

2.5. Heat transfer parameters

The overall Nusselt number for a differentially heated enclosure is evaluated as

$$Nu_0 = \frac{\int_0^H -k(\partial T/\partial x)_H \,dy}{\int_0^H -k(\partial T/\partial x)_c \,dy} = \int_0^1 -(\partial T_*/\partial x_*)\,dy_* \tag{18}$$

where the subscript c refers to the pure conduction situation (i.e. stagnant fluid), and $(\partial T/\partial x)_H$ refers to the temperature gradient in the x-direction calculated at the $x_* = 0$ hot wall. The overall heat transfer across the cavity, when the diffusive inserts at the corners are in place, should consider the heat transfer occurring within the inserts, both for the convective as well as for the pure conduction situation. However, for practical reasons, the reference pure conduction situation is taken as the one corresponding to the enclosure without inserts completely filled with stagnant fluid. This leads to

$k(H \times 1)(T_H - T_C)/H$. This reference situation is well suited for comparison purposes, as it is the usual reference for the overall Nusselt number definition in enclosures [2,14]. The overall heat transfer corresponding to the convective situation can be evaluated as the heat input to the cavity, both through the fluid and through the solid inserts, as the horizontal upper and lower walls are adiabatic.

2.6. Numerical modelling

The set of differential equations (Eqs. (5)–(9)) is solved using an equal order two-dimensional control volume based finite element method, which is a two-dimensional version of the one described in [22]. This method leads to very reliable solutions for this kind of problems. Over the fluid–solid interfaces, the conjugated heat transfer problem is solved by using a constant diffusion coefficient over each finite element. This practice is made possible by matching the mesh to the inserts [22].

Several grid convergence independence tests were conducted, and a 51×51 uniform grid over the fluid domain and the solid inserts offered a good compromise between computational efficiency and grid independence. The accuracy and suitability of this grid were assessed by comparing the results against those of the benchmark solution for the single square enclosure natural convection heat transfer problem [3], and the maximum deviation was less than 2%.

3. Results and analysis

3.1. Values for the dimensionless parameters

Four dimensionless parameters, as already mentioned, govern the conjugated heat transfer problem under consideration, namely: The Prandtl number, Pr, the H-based Rayleigh number, Ra_H, the thermal conductivity ratio, Rc, and the dimensionless length of the solid inserts, d_*. The enclosure is filled with air, with an average value for Pr of 0.73, therefore the effect upon the heat transfer rate of the three dimensionless parameters, and the different combinations for the inserts placement at the corners of the square enclosure are required for the analysis of the problem. The results are presented for three different combinations of the inserts placement, and they were obtained for $Ra_H = 10^4$, 10^5 and 10^6, which are typical values of this parameter for this kind of enclosures. The values of Rc were selected as 1, 10, 100 and 1000. The dimensionless length of the solid inserts was taken in a range of interest from $d_* = 0$ (no inserts) to $d_* = 0.32$.

The main objective under analysis is the overall thermal performance of the enclosure, given by the overall Nusselt number, Nu_0, defined by Eq. (18). All the reported changes in this Nu_0 parameter are relative to the Nusselt number of the single square enclosure, i.e. without inserts at the corners.

3.2. Common trends on the obtained results

The analysis of the results reveals common trends in what concerns the variation of the overall Nusselt number with respect to the thermal conductivity ratio and the dimension of the inserts, as shown in Fig. 2(a)–(c) for $Ra_H = 10^4$, in Fig. 3(a)–(c) for $Ra_H = 10^5$, and in Fig. 4(a)–(c) for $Ra_H = 10^6$.

For each value of the Rayleigh numbers studied, corresponds the overall Nusselt number for the single enclosure situation with no inserts, namely $Nu_0 = 2.24$ for $Ra_H = 10^4$, $Nu_0 = 4.52$ for $Ra_H = 10^5$ and $Nu_0 = 8.77$ for $Ra_H = 10^6$.

As expected, for $Rc = 1$, the overall Nusselt number decreases as d_* increases. In fact, increasing d_* for $Rc = 1$ progressively leads to a pure conduction situation (i.e. stagnant medium condition), and, in the limit, $Nu_0 \equiv 1.00$ for $d_* = 1.00$. This decreasing behaviour of the overall Nusselt number was for all cases studied when $Rc = 1$. This finding causes no surprise, as with $Rc = 1$, increasing value of d_* yields progressive suppression of the convective effects, i.e. for $Ra_H = 10^4$, for instance and for d_* higher than $\sim$0.10 the difference between $\sim$2.24 and subsequent values of Nu_0 indicate a reduction of the heat transfer rate by convection. For inserts made out of materials, which yield values of Rc less than one, the heat transfer rate will also decrease with the increasing size of the insert (i.e. $d_* > 0$).

Another common characteristic is that, for $Rc > 1$, increases on the insert length yield invariably increases of the overall Nusselt numbers. Higher values of Rc, as expected, result in higher values of Nu_0. This effect, however, is more pronounced for small values of Rc, and essentially ceases to exist for values of Rc greater than 100. In fact, there are only slight changes on the overall Nusselt number when Rc changes from 100 to 1000, thus indicating an asymptotic behaviour of the Nusselt number with the limit corresponding to the results for values of Rc close to 100. Moreover, the change of the overall Nusselt number caused by varying Rc from 100 to 1000 is relatively insensitive to the value of Ra_H. This means that inserts of high thermal conductivity increase the overall thermal performance of the enclosure, and that there are no significant increases in the thermal performance for insert materials with $k_w/k \geqslant 100$. Therefore, with $k \approx 0.026$ W/(m K) for air, a reasonably good value for the thermal conductivity of the inserts would be $k_w \approx 2.6$ W/(m K), a value which corresponds to many metallic materials, or even non-metallic materials such as, for example, refractory materials, magnesite brick, some rocks or silicon.

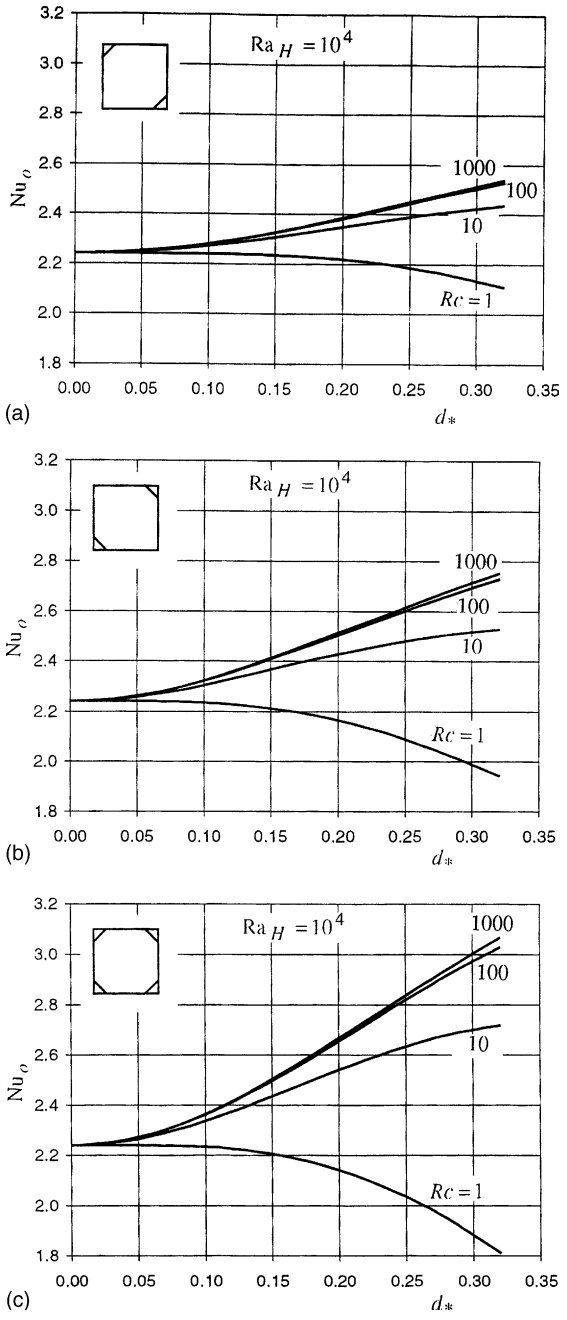

Fig. 2. Nusselt number variation with length of the inserts and with the thermal conductivity ratio for the square enclosure with $Ra_H = 10^4$ for: (a) inserts placed at the upper-left and lower-right corners; (b) inserts placed at the lower-left and upper-right corners; and (c) inserts placed at all the corners.

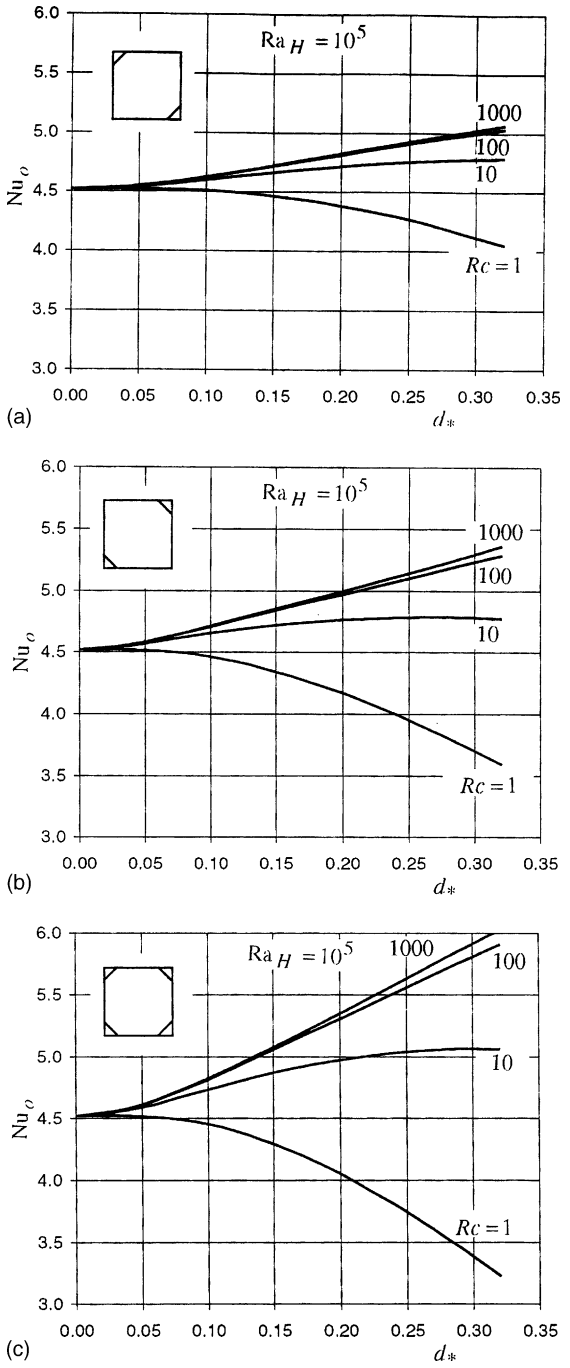

Fig. 3. Results for the square enclosure with $Ra_H = 10^5$. Remaining caption as for Fig. 2.

For $Rc = 100$ and 1000, the Nusselt number increases almost linearly with d_*, for $d_* > 0.10$. For $Rc = 10$ the Nusselt number increases with d_*, and it is strongly dependent of the Rayleigh number. For $Rc = 10$ and $Ra_H = 10^6$ a maximum value of the overall Nusselt number occurs for a particular value of d_*, which is dependent upon the particular placements of the inserts.

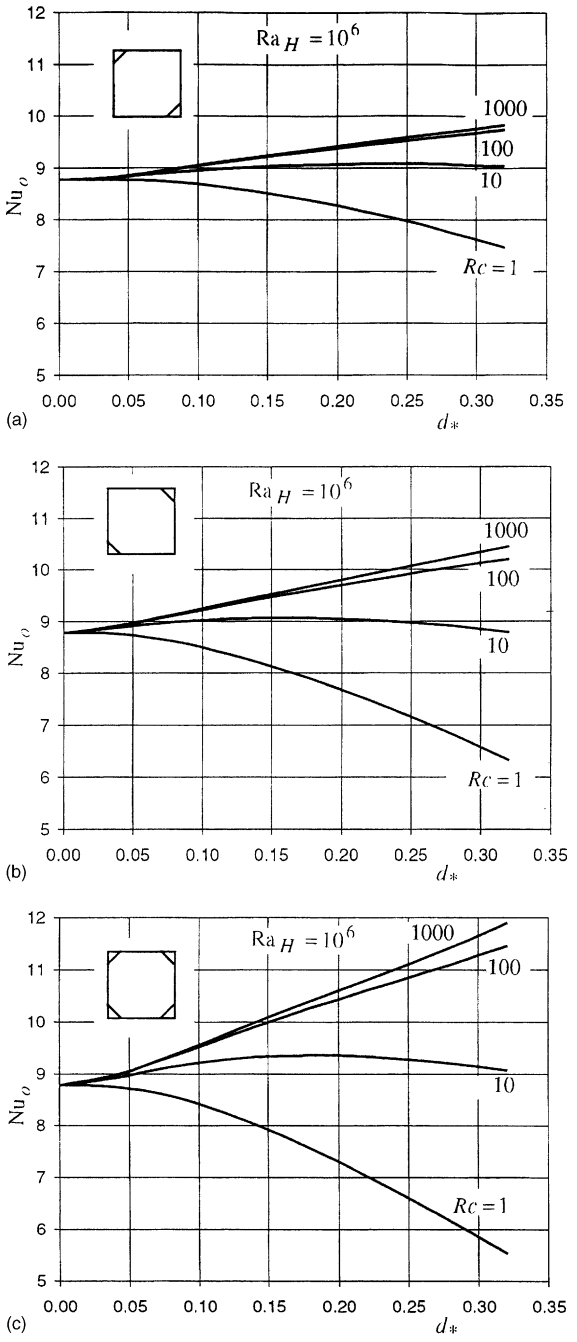

Fig. 4. Results for the square enclosure with $Ra_H = 10^6$. Remaining caption as for Fig. 2.

3.3. Results for the enclosure with inserts at the upper-left and lower-right corners

Fig. 2(a), for $Ra_H = 10^4$, clearly indicates that an increase of the insert length, for $Rc > 1$, yields increasing values of the overall Nusselt number, a trend which is also observed when Rc increase. The predicted increases on the overall Nusselt number, for the limit of $d_* = 0.32$, are of 8.7% for $Rc = 10$, 12.9% for $Rc = 100$ and 13.3% for $Rc = 1000$. For $Rc = 1$, and over the range of values considered for d_*, the decrease of the Nusselt number is of 5.8%. Figs. 3(a) and 4(a) for Ra_H of 10^5 and 10^6, respectively, show similar trends to those described for Fig. 2(a). Increasing values of Ra_H tend to increase slightly the effect of Rc upon the overall Nusselt number, namely with $Ra_H = 10^5$: 5.9% for $Rc = 10$, 11.3% for $Rc = 100$ and 12.1% for $Rc = 1000$; with $Ra_H = 10^6$: 11.0% for $Rc = 100$ and 12.1% for $Rc = 1000$, taking for each of the two cases $Rc = 1$ as the base case. At $Ra_H = 10^6$, due to the increased flow intensity is observed for $Rc = 10$ a maximum Nu_0 of 9.08 for $d_* = 0.24$. For both cases, $Ra_H = 10^5$ and $Ra_H = 10^6$, over the range of values of d_* the maximum decrease of the Nusselt number is 10.3% and 14.8%, respectively, for $Rc = 1$.

With the objective of giving an in-depth physical picture of the problem under consideration the dimensionless velocity and temperature fields for $Ra_H = 10^6$ and inserts of length $d_* = 0.32$ placed at the upper-left and lower-right corners, are shown in Fig. 5(a) and (b) for $Rc = 1$, and in Fig. 6(a) and (b) for $Rc = 10$. The observations for the velocity and temperature fields are essentially similar for the remaining cases.

In what concerns the flow field, the inserts produce some 'realignment' on the streamlines, and the resulting 135° corners yield lower blockages on the flow than those for the original 90° angles of the enclosure without inserts. This simple geometrical argument is corroborated by the results: the inserts enhance the flow within the enclosure, and as a consequence, the overall Nusselt number is also increased. Therefore, the inserts, in this situation, act as heat transfer promoters. The observed structure of the flow field remains essentially the same for both situations of $Rc = 1$ (Fig. 5(a)) and $Rc = 10$ (Fig. 6(a)).

In what concerns the temperature field, it can be noted a marked thermal stratification at the center of the enclosure, the isotherms being clearly flat in this region, both for $Rc = 1$ (Fig. 5(b)) and $Rc = 10$ (Fig. 6(b)). This thermal stratification is a characteristic of the temperature fields for this type of problems, at this level of the Rayleigh number. It should be mentioned that similar behaviour is observed for enclosures without inserts at the corners [3]. For $Rc = 1$, as depicted in Fig. 5(b), the isotherms spread over the solid inserts, thus giving rise to lower temperature gradients near the upper-right and lower-left corners. Lower temperature gradients lead to lower Nusselt numbers, as it will be discussed. For $Rc = 10$ (Fig. 6(b)), the relatively high thermal conductivity of the solid inserts forces the isotherms toward the opposite horizontal corner, resulting in higher thermal gradients near the upper-right and lower-left corners,

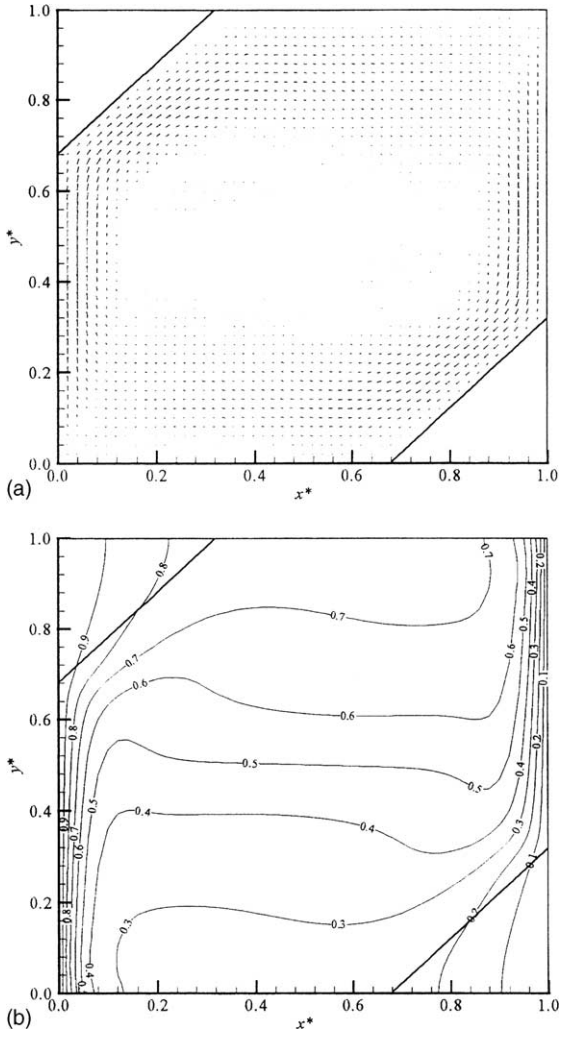

Fig. 5. Results for the enclosure with solid inserts placed at the upper-left and lower-right corners, for $Ra_H = 10^6$, $d_* = 0.32$, and $Rc = 1$: (a) dimensionless velocity field; and (b) dimensionless isotherms.

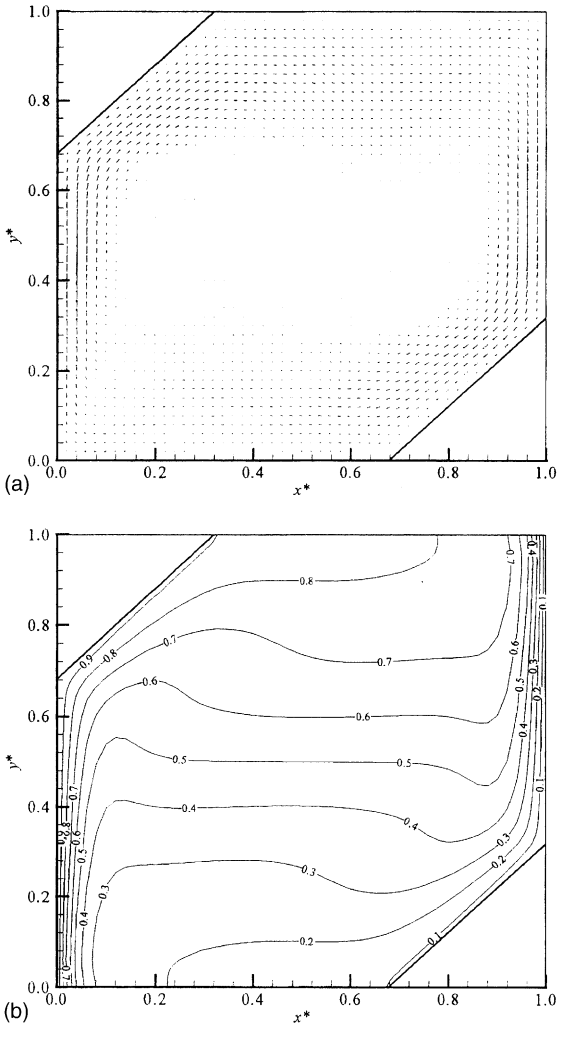

Fig. 6. Caption as for Fig. 3, but for $Rc = 10$.

and in higher Nusselt numbers. Moreover, for relatively high conductivity solid inserts, the "*hot wall*" and the "*cold wall*" contacting the fluid increase in length, its effective length being nearly $H - d + \sqrt{2}d = H + 0.44d$. This effect also leads to enclosures with better thermal performance when acting as heat transfer promoters.

3.4. Results for the enclosure with inserts at the lower-left and upper-right corners

The results obtained for inserts located at the lower-left and upper-right corners, and for $Ra_H = 10^4$, are shown in Fig. 2(b). They present similar behaviour to that previously observed for the enclosure with inserts at the upper-left and lower-right corners. For this particular situation, for $d_* = 0.32$ it is noticed an increase for the Nusselt number of 12.9% for $Rc = 10$, 21.9% for $Rc = 100$ and 22.9% for $Rc = 1000$. It is also observed, as d_* increases, the profile flattens for $Rc = 10$. The maximum observed decrease in the Nusselt number, for $Rc = 1$, when d_* varies from 0 to 0.32, is 13.2%.

The case for $Ra_H = 10^5$ is presented in Fig. 3(b). In this case, the increases of the overall Nusselt number are of: 5.7% for $Rc = 10$, 17% for $Rc = 100$ and 18.6% for $Rc = 1000$. For $Rc = 10$ it is observed a maximum Nusselt number, $Nu_0 = 4.79$, for $d_* = 0.28$. The maximum observed decrease in the Nusselt number is of 20.4%, for $Rc = 1$ and for d_* varying from 0 to 0.32.

The results for $Ra_H = 10^6$ are presented in Fig. 4(b). It is observed a similar behaviour for $Rc = 100$ and $Rc = 1000$ cases. The augmentation on the overall Nusselt number is of 16.3% for $Rc = 100$ and 19.1% for

$Rc = 1000$. For $Rc = 10$, there is a maximum $Nu_0 = 9.06$ for $d_* = 0.16$. The maximum decrease in the Nusselt number, for $Rc = 1$, is of 27.8%.

Altogether, it can be concluded that the inserts placed at the lower-left and upper-right corners, and acting as heat transfer promoters ($Rc > 1$), yield enclosures with better performance than those with the inserts placed at the upper-left and lower-right corners. In what concerns the decrease of the overall Nusselt number, suitable for enclosures acting like thermal insulators ($Rc < 1$), it is also a better practice the placement of the solid inserts at the lower-left and upper-right corners.

3.5. Results for the enclosure with inserts at all corners

For $Ra_H = 10^4$ with inserts at all corners, it can be observed from Fig. 2(c) an increase on the Nusselt number of 21.4% for $Rc = 10$, 35.2% for $Rc = 100$ and 36.9% for $Rc = 1000$. It is also observed a marked tendency toward to a flat profile for $Rc = 10$ as d_* increases. The maximum decrease in the Nusselt number is of 19.0% for $Rc = 1$, and with d_* varying from 0 to 0.32.

The situation for $Ra_H = 10^5$ is presented in Fig. 3(c), where it can be observed essentially the same behaviour as for the enclosure with inserts at the upper-left and lower-right corners. In this case, the increases of the overall Nusselt number are of: 12.0% for $Rc = 10$, 30.7% for $Rc = 100$ and 33.4% for $Rc = 1000$. It is also observed that the profile for $Rc = 10$ is essentially flat for $d_* = 0.32$. The maximum observed decrease in the Nusselt number is of 28.5% in this case.

The results for $Ra_H = 10^6$ are presented in Fig. 4(c). There is a strong increase on the overall Nusselt number, which is of 30.6% for $Rc = 100$ and of 35.6% for $Rc = 1000$. For $Rc = 10$, there is a marked maximum, $Nu_0 = 9.36$, for $d_* = 0.20$.

The main finding is that the inserts placed at all the inner corners yield the best thermal performance among the configurations studied either with the enclosure acting as an heat transfer promoter ($Rc > 1$) or as an insulator ($Rc < 1$). It should be noted also that, for relatively high conductivity solid inserts, the effective hot and cold wall length contacting the fluid is nearly $H - 2d + 2\sqrt{2}d = H + 0.88d$.

4. Conclusions

This work presents a numerical study concerning the use of solid inserts placed at the inner corners of differentially heated square enclosures and its influence on the overall thermal performance of such enclosures. The study was limited to square enclosures and to a limited set of the dimensionless governing parameters. Notwithstanding, similar results would be expected for rectangular enclosures with aspect ratios close to unity.

Square enclosures acting as enhanced thermal insulators, suitable, for example, in some construction elements, can be obtained with inserts of low thermal conductivity. In the limit, their thermal conductivity will be of the same order of magnitude of the thermal conductivity of the fluid that fills the cavity. Significant improvements on the thermal performance of the enclosure can be obtained with considerably small inserts of low thermal conductivity materials, with reductions in the heat transfer crossing the enclosure as high as 27.8% for the cases studied.

On the other hand, square enclosures acting like heat transfer promoters can be obtained through the use of solid inserts made of materials with high or even with moderate thermal conductivity. Results indicate that good results can be obtained with relatively small length inserts, with a thermal conductivity of the order of magnitude of 100 times the thermal conductivity of the air. Above this value, improved thermal conductors lead to only slightly improvements of overall thermal performances of the enclosures. For the cases studied, increases as high as 35.6% are observed for the overall Nusselt number.

The placement and number of solid inserts are important factors, which can affect significantly the thermal performance of the enclosure. The best configuration was, in terms of thermal performance (as an insulator or heat transfer promoter), found to be the one consisting of solid inserts placed at all the inner corners of the enclosure.

A common result is that longer inserts lead to the best performing enclosures, either acting as thermal insulators or as heat transfer promoters. Such devices can be seen as alternatives to the enclosure partitions, in what concerns insulation performance. They do not provide, however a universal solution to increase the global thermal enclosure performance when acting as a heat transfer promoter. A remarkable finding is the fact that some combinations of the dimensionless governing parameters lead to relative maxima on the heat transfer crossing the cavity. This particular result may prove to be of interest toward the design process.

References

[1] K.T. Yang, Natural convection in enclosures, in: S. Kakac, R.K. Shah, W. Aung (Eds.), Handbook of Single Phase Convective Heat Transfer, Wiley, New York, 1987 (Chapter 13).

[2] A. Bejan, Convection Heat Transfer, second ed., Wiley, New York, 1995 (Chapter 5).

[3] G. de Vahl Davis, Natural convection of air in a square cavity: A bench mark numerical solution, Int. J. Numer. Methods Fluids 3 (1983) 249–264.

[4] E. Nobile, A.C.M. Sousa, G.S. Barozzi, Two-equation turbulence modelling in confined free convection, in:

Proceedings Eurotherm Seminar Nr. 11, Natural Convection Enclosures, Harwell Laboratory, UK, December 7–8, 1989, pp. 31–43.
[5] J. Ede, Advances in free convection, in: Advances in Heat Transfer, Academic Press, New York, 1976, pp. 1–64.
[6] N.N. Lin, A. Bejan, Natural convection in a partially divided enclosure, Int. J. Heat Mass Transfer 26 (1983) 1867–1878.
[7] T. Nishimura, F. Nagasawa, Y. Kawamura, Natural convection in horizontal enclosures with multiple partitions, Int. J. Heat Mass Transfer 32 (1989) 1641–1647.
[8] F. Moukalled, S. Acharya, Buoyancy-induced heat transfer in partially divided trapezoidal cavities, Numer. Heat Transfer, Part A 32 (1997) 787–810.
[9] F. Moukalled, S. Acharya, Natural convection in trapezoidal cavities with baffles mounted on the upper inclined surfaces, Numer. Heat Transfer, Part A 37 (1997) 545–565.
[10] K.C. Chung, L.M. Trefethen, Natural convection in a vertical stack of inclined parallelogrammic cavities, Int. J. Heat Mass Transfer 25 (1982) 277–284.
[11] V.A.F. Costa, A.R. Figueiredo, L.A. Oliveira, Convecção natural em navidades paralelográmicas, in: Proceedings of the I Congreso Iberoamericano de Ingeniería Mecánica, vol. 2, E.T.S. Ingenieros Industriales, Madrid, 1993, pp. 255–260.
[12] E.K. Lakhal, M. Hasnaomi, E. Bilgen, P. Vasseur, Natural convection heat transfer in rectangular enclosures with perfectly conduction fins attached to the hot wall, in: Proceedings of the 10th International Heat Transfer Conference, Brighton, UK, 1994, vol. 7, pp. 97–102.
[13] Y.S. Sun, A.F. Emery, Effects of wall conduction, internal heat sources and an internal baffle on natural convection heat transfer in a rectangular enclosure, Int. J. Heat Mass Transfer 40 (4) (1997) 915–929.
[14] V.A.F. Costa, Double diffusive natural convection in a square enclosure with heat and mass diffusive walls, Int. J. Heat Mass Transfer 40 (17) (1997) 4061–4071.
[15] V.A.F. Costa, Natural convection in differentially heated rectangular enclosures with vertical diffusive walls, Int. J. Heat Mass Transfer 45 (20) (2002) 4217–4220.
[16] H.S. Kwak, K. Kuwahara, J.M. Hyun, Resonant enhancement of natural convection heat transfer in a square enclosure, Int. J. Heat Mass Transfer 41 (18) (1998) 2837–2846.
[17] H.S. Kwak, K. Kuwahara, J.M. Hyun, Prediction of the resonance frequency of natural convection in an enclosure with time-periodic heating imposed on one sidewall, Int. J. Heat Mass Transfer 41 (20) (1998) 3157–3160.
[18] E. Nobile, A.C.M. Sousa, G.S. Barozzi, Turbulence modelling in confined natural convection, Int. J. Heat Technol. 7 (3–4) (1989) 24–35.
[19] E. Nobile, A.C.M. Sousa, An implicit scheme for the numerical simulation on time dependent convection in side-heated cavities, in: Y.W. Skin, et al. (Eds.), PVP-VM-270 Transient Thermal Hydraulic, Heat Transfer, Fluid Structure Interaction, and Structural Dynamics, ASME, 1994, pp. 29–37 (book no. G00838).
[20] V.S. Arpaci, P.S. Larsen, Convection Heat Transfer, Prentice-Hall, Englewood Cliffs, NJ, 1984.
[21] D.D. Gray, A. Giorgini, The validity of the Boussinesq approximation for liquids and gases, Int. J. Heat Mass Transfer 19 (5) (1976) 545–551.
[22] V.A.F. Costa, L.A. Oliveira, A.R. Figueiredo, A control volume based finite element method for three-dimensional incompressible turbulent fluid flow, heat transfer, and related phenomena, Int. J. Numer. Methods Fluids 21 (7) (1995) 591–613.